JACS
JOURNAL OF THE AMERICAN CHEMICAL SOCIETY
Article
Cite This: J. Am. Chem. Soc. XXXX, XXX, XXX−XXX
pubs.acs.org/JACS

Synthesis, Characterization, and Reactivity of Complex Tricyclic Oxonium Ions, Proposed Intermediates in Natural Product Biosynthesis

Hau Sun Sam Chan,[†] Q. Nhu N. Nguyen,[†] Robert S. Paton,*[,†,‡] and Jonathan W. Burton*[,†]

[†]Chemistry Research Laboratory, University of Oxford, Mansfield Road, Oxford OX1 3TA, U.K.
[‡]Department of Chemistry, Colorado State University, Fort Collins, Colorado 80523, United States

Supporting Information

ABSTRACT: Reactive intermediates frequently play significant roles in the biosynthesis of numerous classes of natural products although the direct observation of these biosynthetically relevant species is rare. We present here direct evidence for the existence of complex, thermally unstable, tricyclic oxonium ions that have been postulated as key reactive intermediates in the biosynthesis of numerous halogenated natural products from *Laurencia* species. Evidence for their existence comes from full characterization of these oxonium ions by low-temperature NMR spectroscopy supported by density functional theory (DFT) calculations, coupled with the direct generation of 10 natural products on exposure of the oxonium ions to various nucleophiles.

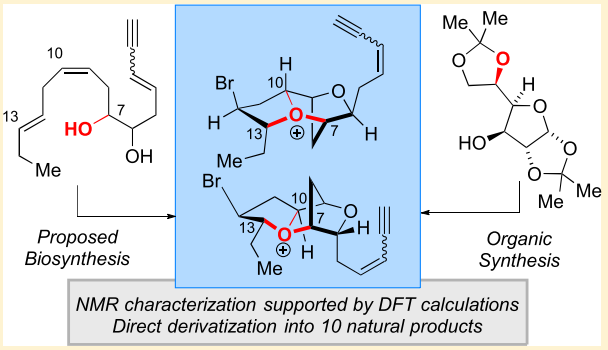

INTRODUCTION

The biosynthesis of secondary metabolites frequently proceeds via unstable reactive intermediates.[1] With terpenes, one of the largest classes of natural products, olefin cyclizations via carbocations (frequently tertiary carbocations) dominate[2−4] and account for the vast structural diversity exhibited by this class of natural products. Evidence for carbocation intermediates has come from many sources[5−7] and is supported by the isolation and condensed phase characterization of tertiary (and other) carbocations (carbenium ions),[8,9] along with numerous biomimetic total syntheses of terpenoid natural products designed so as to proceed via cationic intermediates.[10] Increasingly, the subtleties of these biosynthetic cyclizations are being probed computationally.[4] In a related manner, the biosynthesis of numerous halogenated acetogenin natural products from *Laurencia* species have been proposed to proceed via complex bi- and tricyclic oxonium ions (Figure 1).[11−21] The existence of these trialkyloxonium ions, as with carbocations in terpene biosynthesis, has been implied from the structural and stereochemical diversity of these natural products[22] and initial biosynthetic studies with isolated enzymes[11,13,23] as well as from a number of elegant biomimetic syntheses primarily from Kim, Snyder, and Braddock that involve ring opening/expansions of in situ generated oxonium ions to give a host of structurally diverse *Laurencia* natural products.[15−21,24−30] However, no direct evidence for the existence of these trialkyloxonium ions has been forthcoming. Herein we report the synthesis and full characterization (both chemically and computationally) of one family of tricyclic trialkyloxonium ions—among the most structurally and stereochemically complex oxonium ions characterized to date.[31] Additionally, the elucidation of the in vitro reactivity profile of the tricyclic oxonium ions has resulted in the total synthesis of more than 10 complex halogenated natural products. This work provides chemical evidence for the existence of complex, halogenated, tricyclic oxonium ions that have been postulated as key reactive intermediates in the biosynthesis of numerous halogenated natural products.

Oxonium Ions in *Laurencia* Natural Product Biosynthesis. Red algae of the genus *Laurencia* and organisms that feed on them produce a vast array of structurally diverse C_{15} halogenated cyclic ether acetogenin natural products[22] which have stimulated synthetic chemists to develop numerous new methods to gain access to these complex secondary metabolites.[22,32] Since Masamune's ground-breaking synthesis of (±)-laurencin ((±)-**4**, Figure 1) reported in the 1970s,[33−35] the syntheses of over 50 cyclic halogenated acetogenin natural products from *Laurencia* spp. have been reported with many targets being synthesized by multiple independent routes.[36−39] Hand-in-hand with the development of the synthetic methodology has been the development of biosynthetic postulates toward these natural products with many of these biosynthetic postulates being rich in oxonium ion chemistry including bicyclic oxonium ions derived from epoxides,[15,16] oxetanes,[19] tetrahydrofurans,[17,18] and oxocenes[21] as well as fused[14,25] and bridged tricyclic oxonium ions.[11−13,20,26] Initial proposals regarding the biosynthesis of C_{15} halogenated acetogenin

Received: July 12, 2019

DOI: 10.1021/jacs.9b07438
J. Am. Chem. Soc. XXXX, XXX, XXX−XXX

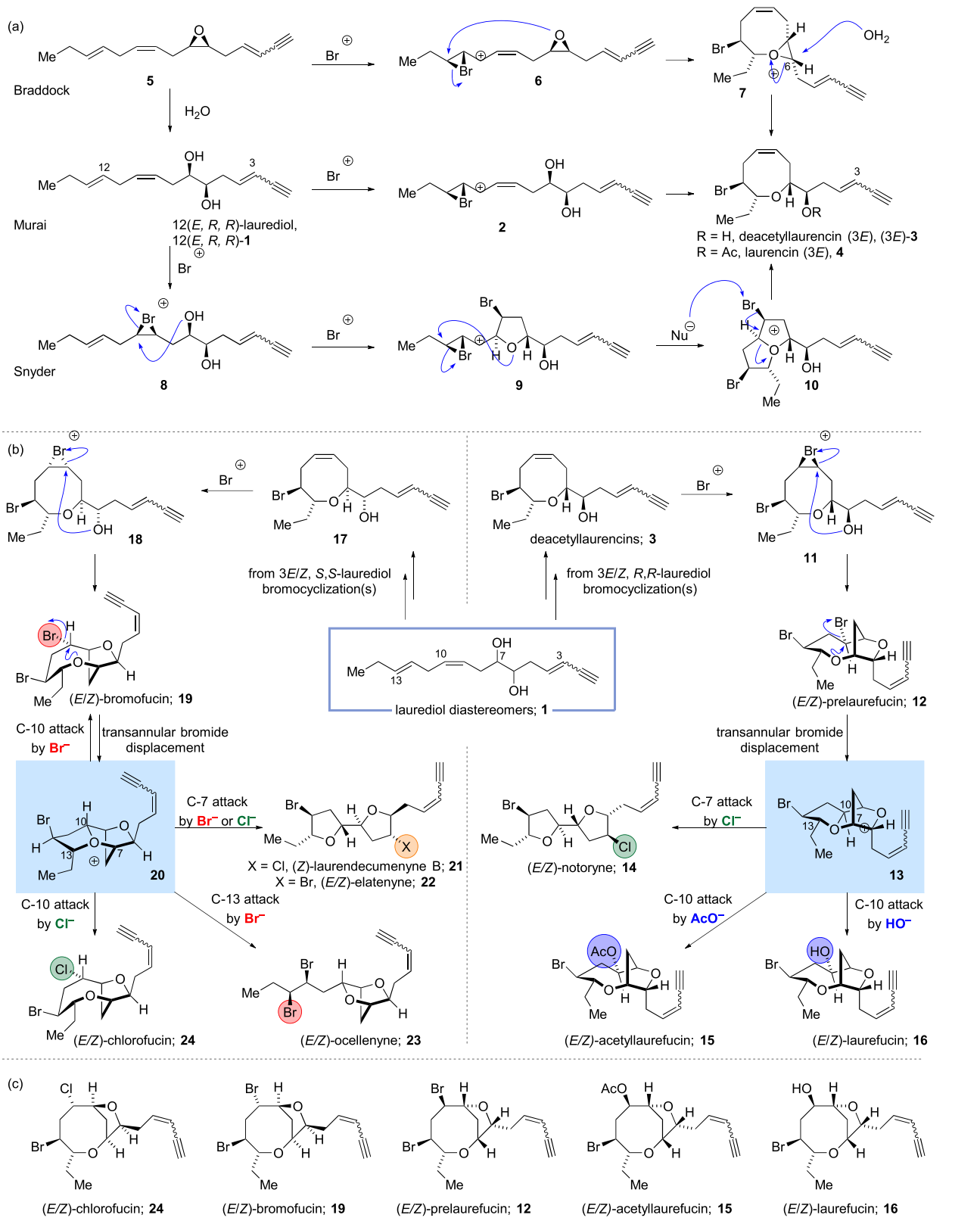

Figure 1. Proposed biosynthesis of some halogenated ethers from *Laurencia* species from laurediols **1**. (a) Proposals regarding the biosynthesis of deacetyllaurencin. (b) Proposed biosynthesis of natural products involving tricyclic oxonium ions. (c) Conventional representations of the lauroxocane natural products the chlorofucins, bromofucins, prelaurefucins, acetyllaurefucins, and the laurefucins.

natural products from *Laurencia* species were put forward by Murai[13,23,40] which involved bromocyclizations of the linear laurediols **1** that exist in nature as mixtures of diastereomers (Figure 1a).[41,42] Murai postulated that enzymatic bromocyclization of the (3*E*,*R*,*R*)-laurediol (3*E*,*R*,*R*)-**1** gives rise to deacetyllaurencin (3*E*)-**3** via bromonium ion **2**;[12,43] indeed, experiments with isolated enzymes yielded deacetyllaurencin (3*E*)-**3** in very low yield (0.015%).[13,23,40,44] More recently,

DOI: 10.1021/jacs.9b07438
J. Am. Chem. Soc. XXXX, XXX, XXX−XXX

trialkyloxonium ions have been proposed as intermediates in the bromocyclization of linear precursors to give deacetyllaurencins **3**. Braddock proposed that laurepoxides **5**, the potential precursor of the lauredials **1**, undergoes bromocyclization to give the bicyclic oxonium ions **7** via the bromonium ions **6**.[15] Opening of the oxonium ions **7** by water at C-6 gives **3**. Such epoxide bromonium ion cyclizations were first reported by Davies with cyclooctadiene epoxide[45] and expanded by Braddock with biosynthetically relevant model systems.[15,16] Snyder has proposed that deacetyllaurencin (3*E*)-**3** could be biosynthesized from (3*E*,*R*,*R*)-lauredials (3*E*,*R*,*R*)-**1** by two favorable 5-endo bromocyclizations via bromonium ions **8** and **9** to give the bicyclic oxonium ion **10** which undergoes formal loss of positive bromine to give deacetyllaurencin (3*E*)-**3**.[17,18] Again, this biomimetic ring expansion of an oxonium ion enjoys experimental support.[17,18,28] In both the Braddock and Snyder proposals the respective oxonium ions can open in other ways to form different ring systems found in other *Laurencia* natural products.

The focus of the current work is the synthesis and characterization of the tricyclic oxonium ions **13** and **20** that are downstream from deacetyllaurencin on the proposed biosynthetic pathway (Figure 1b). Suzuki[12] and Murai and Fukuzawa[11,13] proposed the intermediacy of the oxonium ions **13** in the biosynthesis of notoryne and the laurefucins. The oxonium ions **13** are proposed to arise by transannular displacement of bromide ion from the prelaurefucins **12** which themselves are derived from bromocyclization of deacetyllaurencins **3** (Figure 1b, right).[46] Opening of the oxonium ions **13** with chloride ion at C-7 or with water at C-10 generates the natural products (*E*/*Z*)-notoryne **14**[11,12,47] and (*E*/*Z*)-laurefucins **16**, respectively.[13,23,48] A closely related natural product, acetyllaurefucin (*E*)-**15**,[49] may arise from opening of the oxonium ions **13** with acetate at C-10 or by acetylation of (*E*)-laurefucin (*E*)-**16**. Extension of this biosynthetic postulate[20,26] provides a route to the natural products the bromo-[50] and chlorofucins[51] **19** and **24**, the elatenynes **22**,[52] and laurendecumenyne B **21**,[53] suggesting the participation of oxonium ions **20** as the key biosynthetic intermediates (Figure 1b, left). Analogous to the formation of oxonium ions **13**, the oxonium ions **20** are proposed to originate from (3*E*/*Z*,*S*,*S*)-lauredials (*S*,*S*)-**1**, via a series of enzymatic bromocyclizations followed by transannular bromide displacement from the bicyclic bromofucins **19**. Opening of the oxonium ions **20** at C-10 or C-7 with bromide or chloride ions would generate the natural products **19**, **21**, **22**, and **24**. Alternatively, opening of **20** with bromide ion at C-13 would give the ocellenyes,[54] the full stereostructures of which have recently been tentatively reassigned based on density functional theory (DFT) calculations and biogenetic considerations as **23**.[12,55]

RESULTS AND DISCUSSION

Our strategy for the synthesis of the key oxonium ions **13** and **20** takes its cue from their proposed biosynthesis. This biomimetic approach involves the transannular displacement of halide from bicyclic halo ethers such as **12**, **19**, or **24** using a silver(I)-mediated halide abstraction. Here, precipitation of the silver halide would provide the necessary thermodynamic driving force to compensate for the expected endothermic nature of the oxonium ion formation. The choice of the counteranion of the silver(I) salt was also essential to the successful synthesis of our target oxonium ions. Since oxonium ions are known to alkylate heteroatoms,[56] the counteranion must be non-nucleophilic to prevent premature reaction with the target oxonium ions. In the event, successful oxonium ion formation and characterization was achieved using the weakly coordinating Krossing's anion $[Al(pftb)_4]^-$ (pftb = perfluoro-*tert*-butoxy)].[57] The synthesis of the oxonium ions required the total synthesis of their potential precursors, namely, the bromo- and chlorofucin natural products **19** and **24**, as well as the prelaurefucins **12** and the corresponding C-10 chlorides the neoprelaurefucins **29** (Scheme 1); the neoprelaurefucins have previously been postulated as natural products based on the proposed biogenesis of the laurefucins.[12,26]

Oxonium Ion Precursor Synthesis. Our route to these compounds proceeded from the enantiopure bromomesylates **25** and **31** which were readily prepared from diacetone-D-glucose (Scheme 1 and Supporting Information, sections 2 and 3, pp S4−S24). The bromomesylate **25** would provide the enantiomer of the oxonium ions **13**, namely, *ent*-**13**, and the bromomesylate **31** would give the oxonium ions **20**. The key step in our synthesis of the oxonium ion precursors involved the generation of the diastereomerically pure bromonium ions **26** and **32** from the bromomesylates **25** and **31**. Thus, exposure of the bromomesylate **25** to titanium(IV) chloride,[58] followed by addition of the chloride scavenger $Ag[Al(pftb)_4]\cdot CH_2Cl_2$,[57] and then excess tetrabutylammonium chloride delivered the corresponding dioxabicyclo[5.2.1]decane **28** in 68% yield. We propose that this complex transformation proceeds by initial bromonium ion formation, using Braddock's procedure,[58] followed by removal of excess chloride on addition of the silver(I) salt. This allows time for the bromonium ion **26** to evolve into the corresponding oxonium ion **27** via 5-endo ring closure.[28] Subsequent addition of excess chloride results in C-10 opening of the oxonium ion **27** to give dioxabicyclo[5.2.1]decane **28**.[59] In a similar manner, exposure of the bromomesylate **31** to titanium(IV), followed by silver(I), and then excess chloride or bromide gave the known dioxabicyclo[5.2.1]decanes **34** and **38**[26] resulting from C-10 opening of the oxonium ion **33** by halide anion, along with the corresponding known inseparable 2,2′-bifuranyls **35** and **39**[20] arising from competitive C-7 oxonium ion opening. The dioxabicyclo[5.2.1]decanes **28**, **34**, and **38** were readily converted into the corresponding oxonium ion precursors, the *ent*-neoprelaurefucins *ent*-(*E*/*Z*)-**29**,[59] and the halofucin natural products (*E*/*Z*)-**19**[59] and (*E*/*Z*)-**24**[59] using standard transformations. Thus, *ent*-(*E*)-neoprelaurefucin *ent*-(*E*)-**29** was synthesized from **28** via a cross metathesis with crotonaldehyde and catalyst **30** followed by a Colvin−Ohira reaction to install the (*E*)-enyne in 44% yield for the two steps.[24] The (*Z*)-diastereomer, *ent*-(*Z*)-**29**, was synthesized from **28** via a four-step route involving oxidative cleavage of the terminal olefin in **28**, (*Z*)-vinyl iodide formation using a Stork−Zhao reaction,[60] Sonogashira cross-coupling, and deprotection. The (*E*)- and (*Z*)-halofucins were prepared from the bromochlorides **34** and **35**, and the dibromides **38** and **39** using closely related procedures. Cross metathesis of an inseparable 7:1 mixture of the bromochlorides **34** and **35** with crotonaldehyde and Grubbs catalyst **30** in dichloromethane at 40 °C gave a 4:1 mixture of separable α,β-unsaturated aldehydes **36** and **37** in 78% overall yield.[20] This change of isomer ratio from 7:1 in the starting materials to 4.2:1 in the products is due to the thermal rearrangement of either **34** or **36** or both (see later) most likely via the corresponding tricyclic oxonium ions. Pure **36** has previously been reported by Kim en route to (*E*)-chlorofucin (*E*)-**24**,[26] and we used

DOI: 10.1021/jacs.9b07438
J. Am. Chem. Soc. XXXX, XXX, XXX−XXX

Scheme 1. Synthesis of the Oxonium Ion Precursors, the Bromo- and Chlorofucins, and the *ent*-Neoprelaurefucins[a]

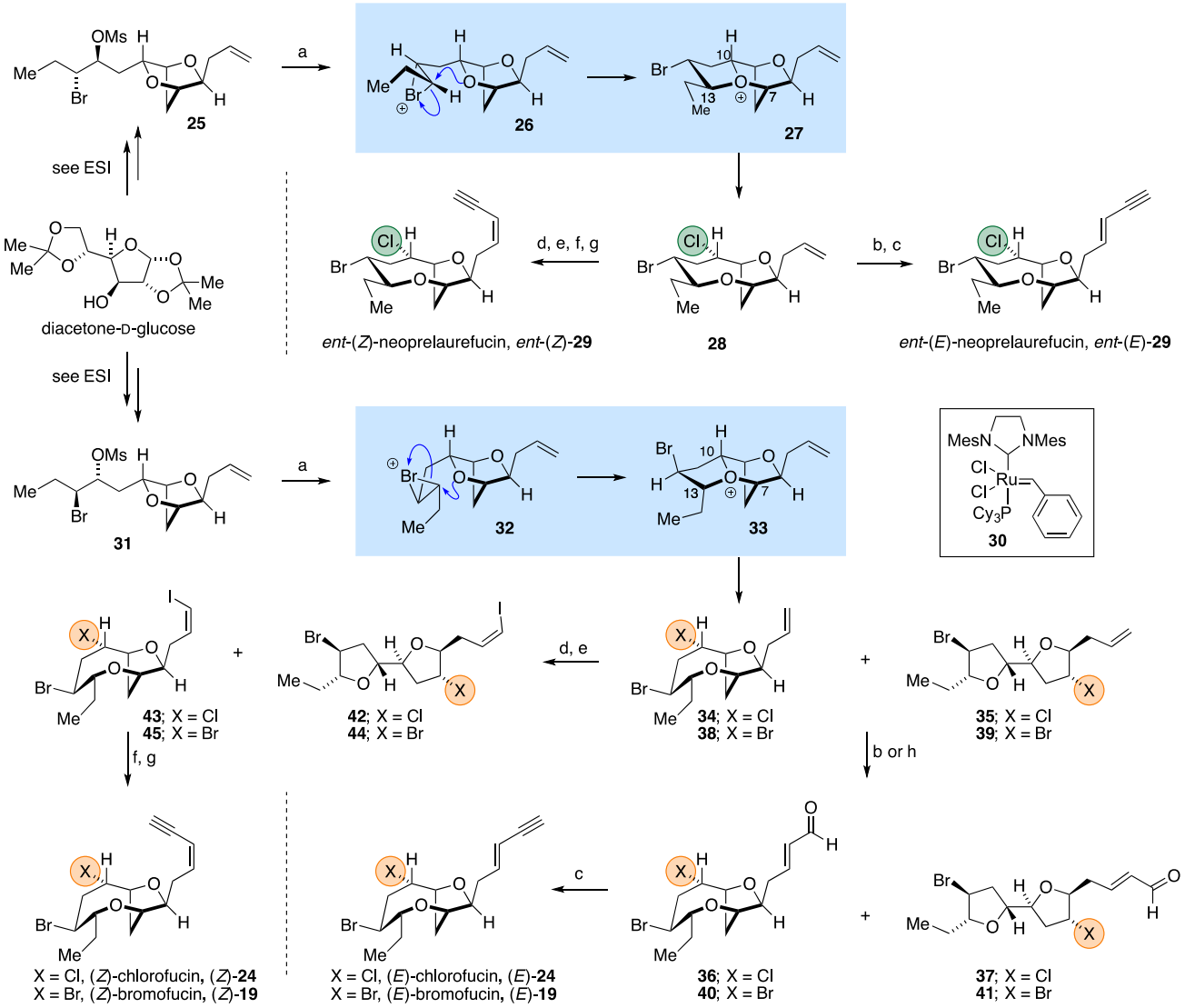

[a]Reagents and conditions: (a) $TiCl_4$, $AgAl(pftb)_4{\cdot}CH_2Cl_2$, CH_2Cl_2 −40 °C, 2 h, and then −78 °C add Bu_4NCl or Bu_4NBr, **28** 68%; **38**:**39** 3:1 inseparable mixture 50%; **34**:**35** 7:1 inseparable mixture 70%; (b) crotonaldehyde, cat. **30**, CH_2Cl_2, 40 °C, **37** 15%, **36** 63%; (c) Me_3SiCHN_2, *n*BuLi, −78 °C−RT, *ent*-(*E*)-**29** 44% (two steps); (*E*)-**19** 42%; (*E*)-**24** 43%; (d) OsO_4, $NaIO_4$, 2,6-lutidine, dioxane, water; (e) ICH_2PPh_3I, NaHMDS, HMPA, THF, −78 °C−RT; (f) $Me_3SiC{\equiv}CH$, $Pd(PPh_3)_4$, CuI, Et_3N; (g) K_2CO_3, MeOH, *ent*-(*Z*)-**29** 20% (four steps); (*Z*)-**19** 17% (four steps); (*Z*)-**24** 32% (four steps); (h) crotonaldehyde, cat. **30**, Cu(I)I, Et_2O, RT, **41** 13%, **40** 60%.

Kim's method to convert **36** into (*E*)-chlorofucin (*E*)-**24**.[24,26] With a mixture of the dibromides **38** and **39**, cross metathesis using the above conditions resulted in the products **40** and **41** being formed as an inseparable mixture with a small amount of the chlorides **36** and **37**. The formation of the chlorides **36** and **37** most likely occurs by oxonium ion formation from **38** or **40** followed by quenching with the chloride from Grubbs second-generation catalyst. Chloride formation could be avoided by conducting the cross metathesis at room temperature in the presence of copper(I) iodide[61] which gave the separable dibromides **40**[26] and **41**[20] in 73% overall yield. Following Kim's precedent, (*E*)-bromofucin (*E*)-**19** was readily prepared from **40** using a Colvin−Ohira homologation.[26] The (*Z*)-halofucins were synthesized from the bromochlorides **34** and **35**, and the dibromides **38** and **39** using a Stork−Zhao olefination[60] to give mixtures of the inseparable vinyl iodides **42** and **43**, and **44** and **45** followed by Sonogashira cross-coupling and deprotection.

Oxonium Ion Synthesis and Characterization. Having secured the synthesis of the oxonium ion precursors, the halofucins **19** and **24** and the enantiomers of the neoprelaurefucins *ent*-**29**, investigation into oxonium ion formation and characterization commenced. Initial experiments demonstrated that a complex tricyclic oxonium ion related to *ent*-**13** was thermally unstable above ca. −40 °C (see Figure 4 below). It was therefore necessary to generate and analyze the oxonium ions at −40 °C or below. Ultimately, we found that exposure of either of the chlorides *ent*-(*E*)-**29** and *ent*-(*Z*)-**29** to $Ag[Al(pftb)_4]{\cdot}CH_2Cl_2$ in CD_2Cl_2 at −78 °C allowed generation of the oxonium ions, *ent*-**13**·$Al(pftb)_4$, which were characterized by NMR at −78 °C after low-temperature filtration of the precipitated silver chloride. The ^1H and ^{13}C NMR spectra of the generated intermediates compared with

DOI: 10.1021/jacs.9b07438
J. Am. Chem. Soc. XXXX, XXX, XXX−XXX

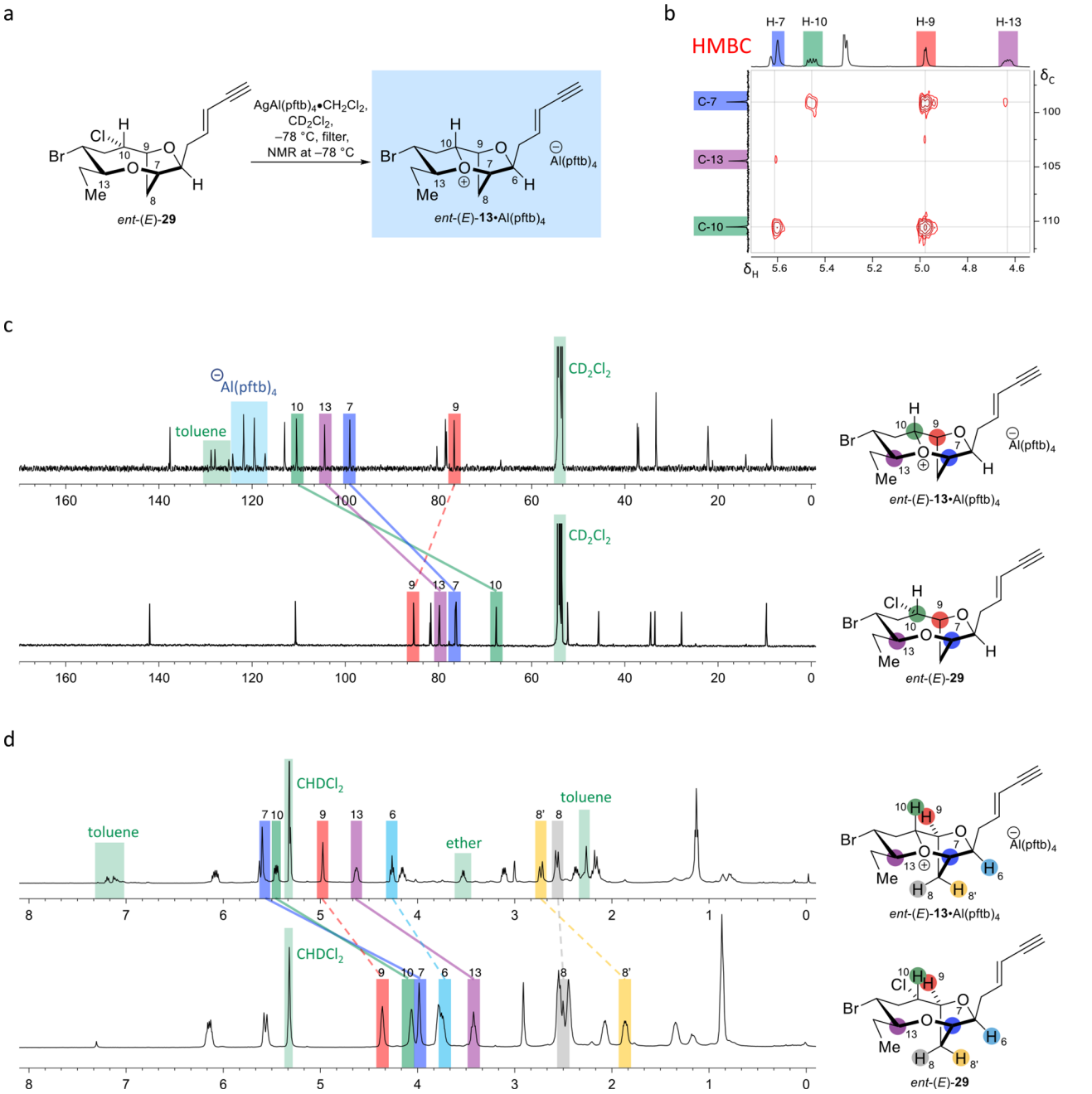

Figure 2. Formation and NMR spectra (CD_2Cl_2, −78 °C) of the oxonium ion *ent*-(*E*)-**13**·Al(pftb)$_4$ along with NMR spectra (CD_2Cl_2, −78 °C) of the starting material *ent*-(*E*)-**29**. The 1-D and 2-D NMR spectra provide evidence for the formation of the oxonium ion *ent*-(*E*)-**13**·Al(pftb)$_4$. In particular, the ^{1}H−^{13}C HMBC spectrum demonstrates the formation of trivalent oxygen. Additionally, on formation of the oxonium ion, the ^{13}C NMR resonances of the carbon atoms directly attached to the trivalent oxygen atom (C-7 blue, C-10 green, and C-13 purple) move to significantly higher chemical shift compared with the starting material, whereas nonadjacent carbons (e.g., C-9 red) undergo smaller changes in chemical shift. The protons adjacent to the trivalent oxygen atom (H-7 blue, H-10 green, and H-13 purple) also move to significantly higher chemical shift on oxonium ion formation. The β-protons (H-6 light blue, H-9 red, and H-8′ yellow) also move to higher chemical shift indicative of overlap of the occupied σ_{C-H} orbital with the σ^*_{C-O} orbital, whereas the gray β-proton (H-8) does not have the correct geometry for σ_{C-H} orbital overlap with the antibonding σ^*_{C-O} orbital and undergoes a significantly smaller change in chemical shift (see the Supporting Information for NBO analysis, Figure S32, pp S102−S103). (a) Formation of the oxonium ion *ent*-(*E*)-**13**·Al(pftb)$_4$ by chloride abstraction from the dioxabicyclo[5.2.1]decane *ent*-(*E*)-**29** at −78 °C. (b) ^{1}H−^{13}C HMBC (heteronuclear multiple bond correlation) NMR spectrum of *ent*-(*E*)-**13**·Al(pftb)$_4$. (c) ^{13}C NMR spectrum of *ent*-(*E*)-**13**·Al(pftb)$_4$ (top) and ^{13}C NMR spectrum of *ent*-(*E*)-**29** (bottom) with corresponding carbons joined by filled lines (carbons α to trivalent oxygen) and dashed lines (carbon β to trivalent oxygen). (d) ^{1}H NMR spectrum of *ent*-(*E*)-**13**·Al(pftb)$_4$ (top) and ^{1}H NMR spectrum of *ent*-(*E*)-**29** (bottom) with corresponding protons joined by filled lines (protons α to trivalent oxygen) and dashed lines (protons β to trivalent oxygen).

those of the precursors, along with the ^{1}H−^{13}C HMBC spectra, provided good evidence for the formation of the oxonium ions, illustrated for *ent*-(*E*)-**13**·Al(pftb)$_4$ in Figure 2. Referring to a section of the ^{1}H−^{13}C HMBC spectrum shown in Figure 2b, the trivalent nature of the oxygen atom within *ent*-(*E*)-**13**·Al(pftb)$_4$ is evident from the correlations of C-7

DOI: 10.1021/jacs.9b07438
J. Am. Chem. Soc. XXXX, XXX, XXX−XXX

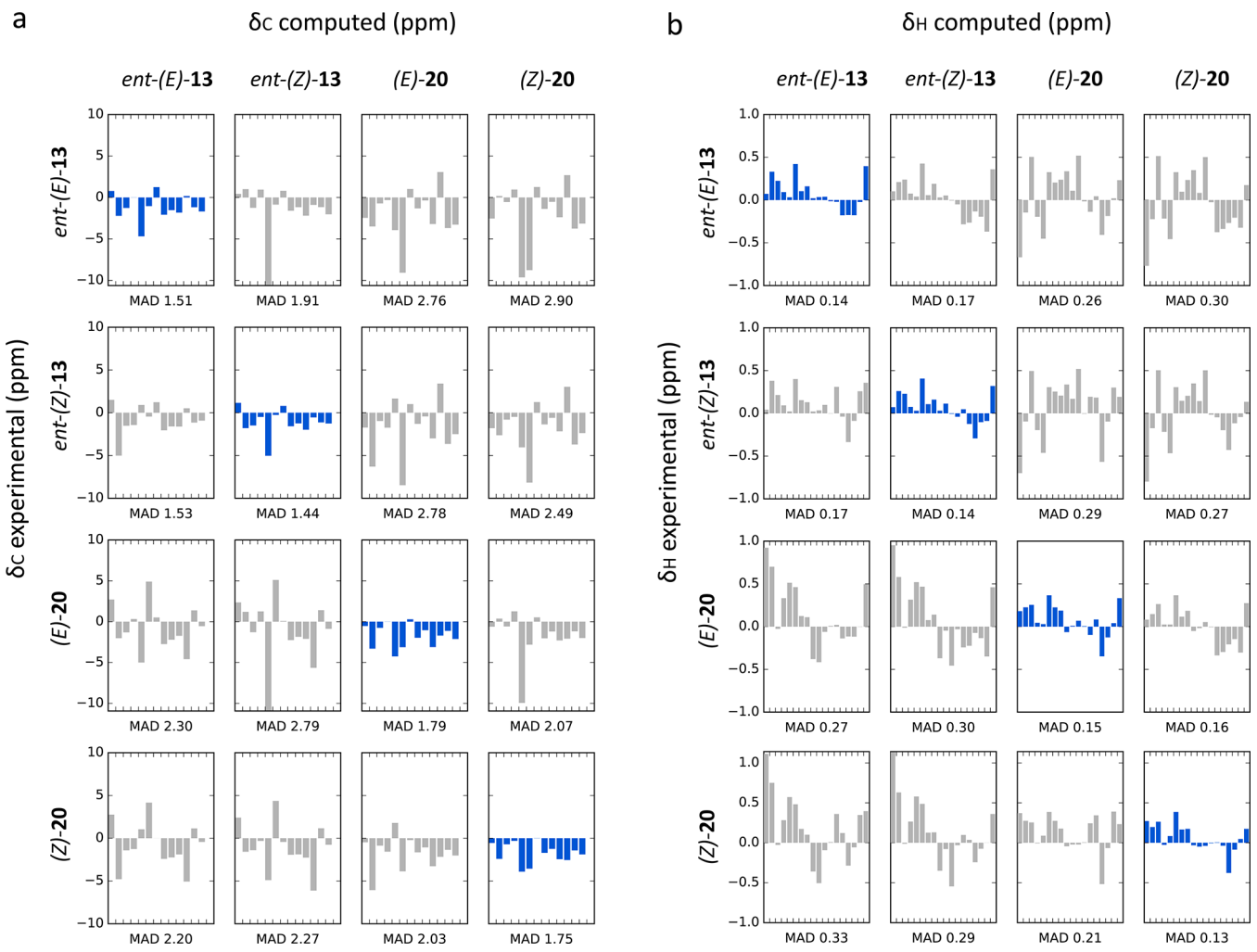

Figure 3. Comparison of experimental and computed ^{13}C and ^{1}H NMR chemical shifts of the oxonium ions *ent*-(*E*/*Z*)-**13** and (*E*/*Z*)-**20**. For each individual histogram, the *x*-axis corresponds to atom number and the *y*-axis corresponds to $\delta_{expt} - \delta_{comp}$. The computed chemical shifts for each oxonium ion are Boltzmann-weighted averages of the chemical shifts from their contributing conformers at −78 °C. (a) Comparison of the experimental and computed ^{13}C NMR chemical shifts of the oxonium ions *ent*-(*E*/*Z*)-**13** and(*E*/*Z*)-**20** (C-4 and C-12 were excluded from the analysis—see the Supporting Information). (b) Comparison of the experimental and computed ^{1}H NMR chemical shifts of the oxonium ions *ent*-(*E*/*Z*)-**13** and(*E*/*Z*)-**20**. The entries highlighted in blue correspond to the least deviation between computed and experimental chemical shifts, having the lowest mean absolute deviation (MAD) as well as the lowest individual deviations in ^{13}C and ^{1}H chemical shifts (Tables S22−S28, pp S89−S95), hence confirming the structural assignment of the oxonium ions.

(blue) to H-10 (green), H-9 (red), and H-13 (purple) as well as from C-10 (green) to H-7 (blue). Additional evidence for the formation of *ent*-**13**·Al(pftb)$_4$ comes from the change in ^{1}H and ^{13}C chemical shifts in moving from *ent*-(*E*)-**29** to the oxonium ion *ent*-(*E*)-**13**·Al(pftb)$_4$. Figure 2c shows clearly that the resonances for C-7 (blue), C-10 (green), C-13 (purple) carbon atoms move to significantly higher chemical shift on treatment of *ent*-(*E*)-**29** with a silver(I) salt, in keeping with the large ^{13}C NMR chemical shift changes observed on oxonium ion formation in other tricyclic systems,[62,63] whereas the resonance for C-9 (red) moves to slightly lower chemical shift. In a similar manner, Figure 2d shows the change in chemical shifts of a number of protons on moving from *ent*-(*E*)-**29** to *ent*-(*E*)-**13**·Al(pftb)$_4$. The protons α to the trivalent oxygen atom, H-7 (blue), H-10 (green), and H-13 (purple) in *ent*-(*E*)-**13**·Al(pftb)$_4$ resonate at significantly higher chemical shift compared with the corresponding protons in *ent*-(*E*)-**29**. The resonances for the β-protons H-6 (light blue), H-9 (red), H-8′ (yellow) also move to higher chemical shift, indicative of overlap of the occupied σ_{C-H} orbitals of H-6, H-9, and H-8′ with the corresponding σ^*_{C-O} orbitals of the trivalent oxygen. The H-8 (gray) proton does not have the correct geometry to maximize this overlap, and hence, its chemical shift remains virtually unchanged (see Figure S32, pp S102−S103 for NBO analysis).[59] In a similar manner, the oxonium ions (*E*)- and (*Z*)-**20**·Al(pftb)$_4$ could be readily generated from the bromofucins **19** and were characterized as above; equivalent figures to Figure 3 for the oxonium ions *ent*-(*Z*)-**13**·Al(pftb)$_4$ and (*E*)- and (*Z*)-**20**·Al(pftb)$_4$ may be found in the Supporting Information (Figures S10−S12, pp S47−S49).

DFT calculated ^{13}C and ^{1}H NMR chemical shifts of the computed structures of each oxonium ion provided further supporting evidence for the formation and structural assignment of the four synthetic oxonium ions *ent*-(*E*/*Z*)-**13**·Al(pftb)$_4$ and (*E*/*Z*)-**20**·Al(pftb)$_4$ (Figure 3). Following a conformational search, Boltzmann-weighted shielding tensors were calculated at the mPW1PW91/6-311+G(2d,p)//B3LYP/6-31+G(d,p) level of theory in dichloromethane, from which

DOI: 10.1021/jacs.9b07438
J. Am. Chem. Soc. XXXX, XXX, XXX−XXX

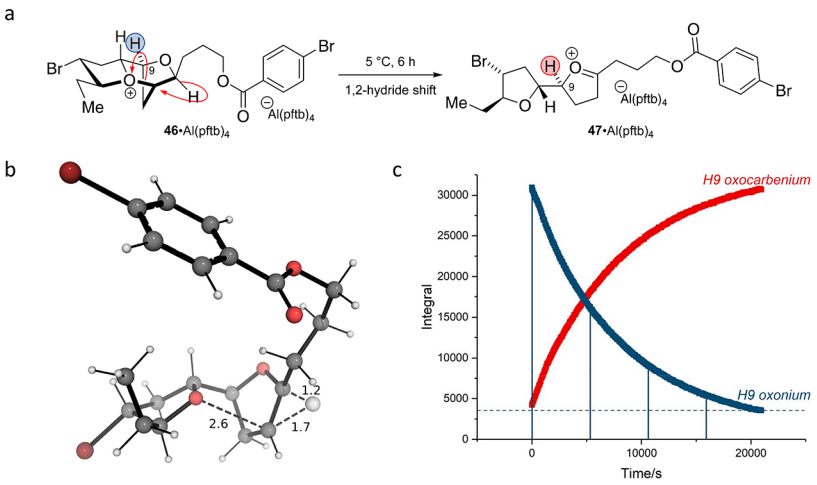

Figure 4. Rearrangement of the oxonium ion **46**·Al(pftb)$_4$ to give the oxocarbenium ion **47**·Al(pftb)$_4$. The stability of the oxonium ion **46**·Al(pftb)$_4$ was quantified by measuring the half-life (ca. 5100 s) for conversion into the oxocarbenium ion **47**·Al(pftb)$_4$ at 5 °C by ^{1}H NMR. The calculated transition state for this rearrangement is a highly asynchronous 1,2-hydride shift. (a) Conversion of **46**·Al(pftb)$_4$ into **47**·Al(pftb)$_4$ with proposed mechanism. (b) DFT calculated transition structure for the conversion of **46** into **47**, distances in angstroms. (c) Plot of the change of the ^{1}H NMR integral for H-9 of **46**·Al(pftb)$_4$ (blue) and H-9 of **47**·Al(pftb)$_4$ (red) vs time, along with half-life intervals on the *x*-axis.

^{13}C and ^{1}H NMR chemical shifts were obtained using the scaling factors reported by Tantillo.[64] For each oxonium ion, the smallest deviation between the experimental chemical shifts and the pool of computed chemical shifts was found only when the configuration of the computed structure matched the configuration of the structure expected from synthesis (diagonals of Figure 3, parts a and b). The off-diagonal entries, which correspond to comparison between structures of different configurations, gave larger mean absolute deviations (MADs) as well as larger deviations of individual ^{13}C and/or ^{1}H NMR chemical shifts. Furthermore, the chemical shifts of the carbon and proton atoms adjacent to the trivalent oxygen were in keeping with simpler tricyclic oxonium ions.[62,63]

Characterization of a Decomposition Pathway. The synthetic oxonium ions *ent*-(*E*)- and *ent*-(*Z*)-**13**·Al(pftb)$_4$ and (*E*)- and (*Z*)-**20**·Al(pftb)$_4$ were thermally unstable and readily decomposed above −40 °C. Indeed, it was not possible to synthesize the oxonium ion (*E*)-**20**·Al(pftb)$_4$ from (*E*)-chlorofucin (*E*)-**24** as the halide abstraction reaction only occurred above −40 °C (for energy profile for oxonium ion formation, see Figures S33−S35, pp S104−S108).[29] The thermal instability of a closely related oxonium ion was studied which resulted in the characterization of a clean decomposition pathway (Figure 4). The oxonium ion **46**·Al(pftb)$_4$ was synthesized at −78 °C by halide abstraction from the corresponding chloride precursor using AgAl(pftb)$_4$·CH_2Cl_2 and characterized by NMR spectroscopy at −78 °C (see the Supporting Information, p S57);[59] the chloride precursor was readily prepared from the alkene **28** by a hydroboration/oxidation/esterification sequence (see the Supporting Information, pp S56−S57). At higher temperature (>−40 °C) the oxonium ion **46**·Al(pftb)$_4$ was readily and cleanly transformed into the oxocarbenium ion **47**·Al(pftb)$_4$ which itself was fully characterized (see the Supporting Information, pp S56−S59). Incubation of the oxonium ion **46**·Al(pftb)$_4$ at 5 °C in an NMR spectrometer allowed the rate of this isomerization to be determined. The half-life for the conversion of **46**·Al(pftb)$_4$ into **47**·Al(pftb)$_4$ at 5 °C was ca. 5100 s (average of three experiments) corresponding to a Gibbs energy of activation of 21.2 kcal/mol. The conversion of **46** into **47** computationally was shown to be a highly asynchronous 1,2-hydride shift with a calculated Gibbs energy barrier of 20.6 kcal/mol, consistent with experiment.[65,66]

Oxonium Ion Reactivity with Nucleophiles. Having characterized the complex halogenated tricyclic oxonium ions both spectroscopically and computationally we sought to investigate their reactivity with a variety of nucleophiles to garner evidence to support their proposed intermediacy in the biosynthesis of *Laurencia* natural products. Trapping of the various oxonium ions with a range of nucleophiles directly generated 10 natural products (Scheme 2). Trapping of the oxonium ions (*E*)- and (*Z*)-**20**·Al(pftb)$_4$ with bromide anion gave rise to the (*E*)- and (*Z*)-bromofucins **19** in 37% and 51% yields, respectively,[26] along with small amounts of (*E*)- and (*Z*)-elatenyne **22**.[20] Using chloride in place of bromide anion gave the corresponding (*E*)- and (*Z*)-chlorofucins **24** in 46% and 63% yields, respectively, along with a trace amount of laurendecumenyne B **21**.[20,26] In the other diastereomeric series, treatment of the oxonium ions *ent*-(*E*)- and *ent*-(*Z*)-**13**·Al(pftb)$_4$ with water gave the corresponding *ent*-laurefucins *ent*-**16** in 34% and 51% yields, respectively.[24,28] Using acetate anion with *ent*-(*E*)-**13**·Al(pftb)$_4$ gave *ent*-acetyllaurefucin *ent*-**15** in 30% yield. Both *ent*-(*E*)- and *ent*-(*Z*)-**13**·Al(pftb)$_4$ were also treated with chloride anion which gave the *ent*-(*E*)- and *ent*-(*Z*)-neoprelaurefucins *ent*-**29** in 59 and 73% yields, respectively.[12,26] What is clear from these quenching experiments is that all four oxonium ions undergo kinetic quenching at C-10 in keeping with results in related systems.[24,26,29,67] Additionally, the oxonium ions (*E*)- and (*Z*)-**20**·Al(pftb)$_4$ undergo a small amount of C-7 quenching analogous to previous work;[26,29,67] in keeping with related results, products from quenching of the oxonium ions at C-13 were not observed.[55] The quenching experiments provided the 2,2′-bifuranyl natural products **21** and **22** in low yields. However, it is known that C-10 halogenated dioxabicyclic compounds related to the halofucins can undergo slow rearrangement to the corresponding 2,2-bifuranyls in the presence of activated silica gel.[12,20,27,48b,67] Hence, exposure of the bromofucins **19** to activated silica gel in hexanes or petroleum ether for 36 h at ambient temperature gave (*E*)- and (*Z*)-elatenyne **22** in 61%

DOI: 10.1021/jacs.9b07438
J. Am. Chem. Soc. XXXX, XXX, XXX−XXX

Scheme 2. Natural Products from Oxonium Ions via Quenching with Nucleophiles[a,b,c]

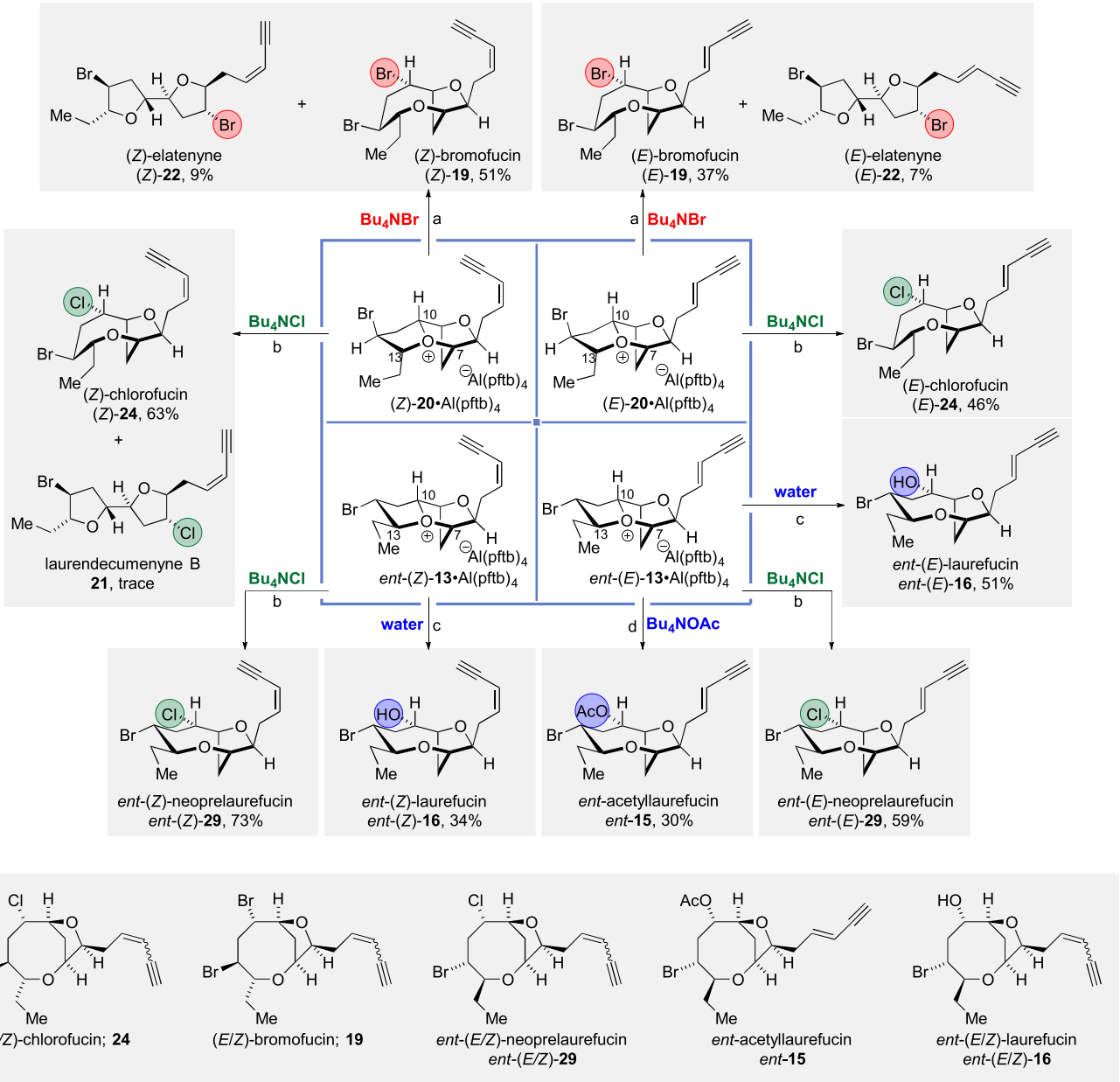

[a]Reagents and conditions: (a) Bu_4NBr, −78 °C−RT, (*Z*)-**19** 51%, (*Z*)-**22** 9%; (*E*)-**19** 37%, (*E*)-**22** 7%; (b) Bu_4NCl, −78 °C−RT, (*Z*)-**24** 63%, **21** trace; (*E*)-**24** 46%; *ent*-(*Z*)-**29** 73%; *ent*-(*E*)-**29** 59%; (c) water, $NaHCO_3$, −78 °C−RT, *ent*-(*Z*)-**16** 34%, *ent*-(*E*)-**16** 51%; (d) Bu_4NOAc, −78 °C−RT, *ent*-**15** 30%. [b]The conventional representations of the lauroxocane natural products, the chlorofucins and bromofucins, and the enantiomers of the neoprelaurefucins, the laurefucins, and acetyllaurefucin are given at the bottom of the scheme. [c]The neoprelaurefucins **29** have previously been predicted to be natural products (refs 12, 26).

and 60% yields, respectively (Scheme 3).[20] In a similar manner, heating (*Z*)-chlorofucin (*Z*)-**24** with activated silica gel in chloroform at 80 °C (bath temperature) gave laurendecumenyne B **21** in 73% yield, while (*E*)-chlorofucin (*E*)-**24** gave (*E*)-laurendecumenyne B (*E*)-**21**, which has yet to be isolated from nature,[20] in 50% yield on exposure to activated silica gel in hexanes at 80 °C (bath temperature).[29] *ent*-(*E*/*Z*)-Neoprelaurefucins *ent*-**29** as solutions in hexanes when treated with silica gel at 80 °C (bath temperature) for 12 h gave *ent*-(*E*)- and *ent*-(*Z*)-notoryne *ent*-**14** quantitatively.[47]

The course of the rearrangement of *ent*-**29** into *ent*-(*Z*)-**14** at 80 °C (bath temperature) in $CDCl_3$ in the absence of silica gel was readily followed by ^1H NMR (see Figure S59, p S206) which indicated clean and quantitative conversion after 12 days.

DFT calculations of transition structures (TSs) helped to explain the observed regioselectivity in the nucleophilic opening of oxonium ions *ent*-(*E*)-**13** and (*E*)-**20**.[25] For *ent*-(*E*)-**13**, the energy barrier for opening at C-10 with chloride is lower than for the corresponding openings at C-7 and C-13 (Figure 5b, also see Figures S36−S48, pp S109−S130 for analyses with different oxonium ions and nucleophiles).[68] The O−C-10 bond is longest in the ground state (Figure 5a), indicative of greater carbocationic character at C-10. Accordingly, attack at this position involves the least structural reorganization in the TS; this can also be quantified through

DOI: 10.1021/jacs.9b07438
J. Am. Chem. Soc. XXXX, XXX, XXX−XXX

Scheme 3. Natural Products from Natural Products[a,b]

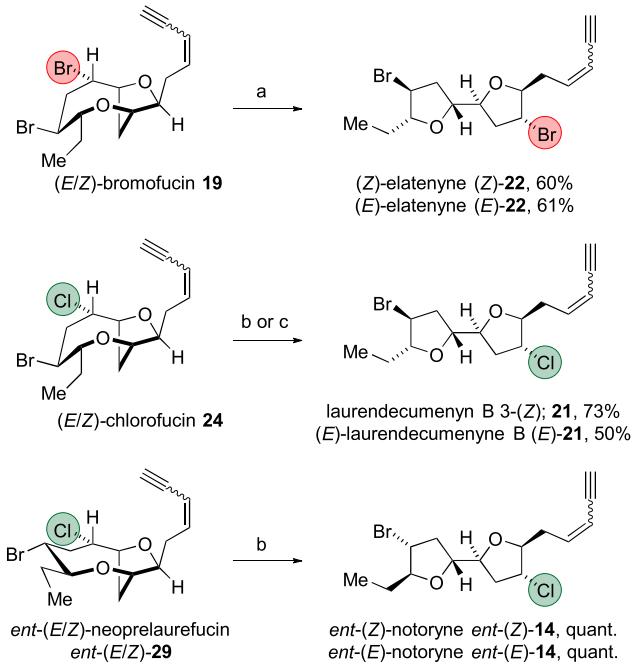

[a]Reagents and conditions: (a) activated silica gel, hexanes or petroleum ether, RT, (*E*)-**22** 61%; (b) activated silica gel, hexanes or petroleum ether, 80 °C (bath temperature), (*Z*)-**22**, 60%; (*E*)-**21** 50%; *ent*-(*Z*)-**14** quant, *ent*-(*E*)-**14** quant; (c) activated silica gel, $CHCl_3$, 80 °C (bath temperature), **21** 73%. [b](*E*)-Laurendecumenyne is likely to be a natural product that is yet to be isolated.

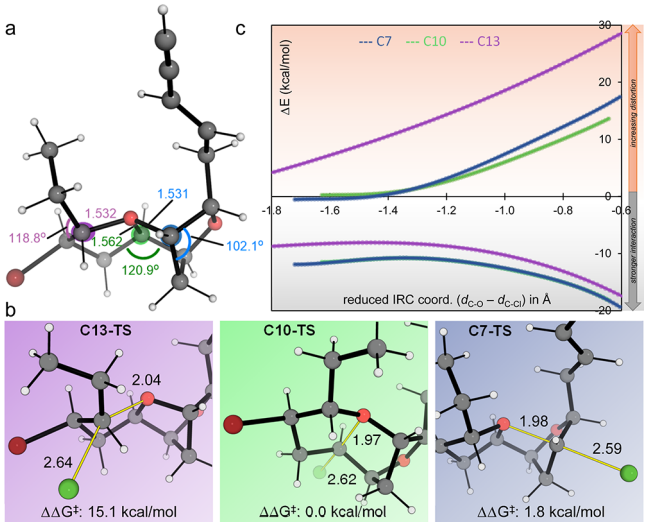

Figure 5. DFT analysis of oxonium ion opening with chloride as nucleophile. (a) The lowest energy conformer of *ent*-(*E*)-**13** and relevant bond lengths and angles; O−C-10 is the longest bond. (b) TSs for opening at C-13, C-10, and C-7. (c) Distortion-interaction/activation-strain analysis along the opening reaction coordinate. The oxonium ion undergoes least distortion when opening at C-10. Distances in angstroms.

distortion-interaction/activation-strain analysis along the reaction coordinate (Figure 5c).[69] Attack at C-7 and C-10 involves very similar interaction energy profiles, while the distortion energy term at C-10 is smaller leading up to the TS, giving rise to a smaller barrier for this position. Consistent with the absence of C-13 opening in our experimental studies, the barrier for attack at this position is much greater than at C-7 and C-10. This principally results from a much larger distortion energy term required to open at this position, also resulting in a later TS with respect to the breaking C−O bond.

Consistent with synthetic studies (Scheme 2), the preferential site of nucleophilic attack by chloride is computed to be C-10, followed by C-7 for both *ent*-(*E*)-**13** and (*E*)-**20**. With water as the nucleophile, the selectivity between C-10 and C-7 for (*E*)-**20** is calculated to be much more finely balanced with $\Delta E^{\ddagger}$ slightly favoring C-10 opening while $\Delta G^{\ddagger}$ slightly favors C-7 opening (Figures S36−S48, pp S109−S130).[29] Regardless, the energetic preference for attack at C-10 over C-7 is relatively modest and could be overcome by the intervention of enzymatic control. The reorganization required for attack at C-13 is substantial for *ent*-(*E*)-**13**, although we found this pathway to be more competitive for (*E*)-**20**; from this oxonium ion, enzymatic promotion of the C-13 pathway is more plausible.[55,70]

CONCLUSION

We have synthesized and characterized four complex halogenated tricyclic oxonium ions (*E*)- and (*Z*)-**20** and *ent*-(*E*)- and *ent*-(*Z*)-**13**, proposed as key reactive intermediates in the biosynthesis of numerous halogenated acetogenin natural products from *Laurencia* spp. using low-temperature NMR experiments and DFT calculations. Furthermore, we have shown that, on exposure to a range of nucleophiles, these oxonium ions directly generate 10 natural products. The above work provides chemical evidence to support the proposed intermediacy of such intermediates biosynthetically and sets the scene for future biosynthetic studies on C-15 halogenated acetogenin natural products.

ASSOCIATED CONTENT

Supporting Information

The Supporting Information is available free of charge on the ACS Publications website at DOI: 10.1021/jacs.9b07438.

Experimental procedures, characterization data, NMR spectra of reported compounds, computational details (PDF)

The *xyz* coordinates of computed structures (ZIP)

AUTHOR INFORMATION

Corresponding Authors

*robert.paton@colostate.edu

*jonathan.burton@chem.ox.ac.uk

ORCID

Robert S. Paton: 0000-0002-0104-4166

Jonathan W. Burton: 0000-0002-5181-5301

Notes

The authors declare no competing financial interest.

ACKNOWLEDGMENTS

We thank the Croucher Foundation for the award of a University of Oxford Croucher Scholarship to H.S.S.C. and Project 752491 from the European Union's Horizon 2020 research and innovation program under the Marie Skłodowska-Curie Grant Agreement No. 752491. We used the RMACC Summit supercomputer, which is supported by the National Science Foundation (ACI-1532235 and ACI-1532236), the University of Colorado Boulder and Colorado State University,

DOI: 10.1021/jacs.9b07438
J. Am. Chem. Soc. XXXX, XXX, XXX−XXX

the Extreme Science and Engineering Discovery Environment (XSEDE) through allocation TG-CHE180056.

REFERENCES

(1) McMurry, J.; Begley, T. *The Organic Chemistry of Biological Pathways*; Roberts and Company: Englewood, CO, 2005.
(2) Tantillo, D. J. The carbocation continuum in terpene biosynthesis—where are the secondary cations? *Chem. Soc. Rev.* **2010**, *39*, 2847−2854.
(3) Dewick, P. M. The biosynthesis of C5−C25 terpenoid compounds. *Nat. Prod. Rep.* **2002**, *19*, 181−222.
(4) Tantillo, D. J. Biosynthesis via carbocations: theoretical studies on terpene formation. *Nat. Prod. Rep.* **2011**, *28*, 1035−1053.
(5) Thulasiram, H. V.; Erickson, H. K.; Poulter, C. D. A common mechanism for branching, cyclopropanation, and cyclobutanation reactions in the isoprenoid biosynthetic pathway. *J. Am. Chem. Soc.* **2008**, *130*, 1966−1971.
(6) Wendt, K. U.; Schulz, G. E.; Corey, E. J.; Liu, D. R. Enzyme Mechanisms for Polycyclic Triterpene Formation. *Angew. Chem., Int. Ed.* **2000**, *39*, 2812−2833.
(7) Christianson, D. W. Structural and Chemical Biology of Terpenoid Cyclases. *Chem. Rev.* **2017**, *117*, 11570−11648.
(8) Olah, G. A.; Tolgyesi, W. S.; Kuhn, S. J.; Moffatt, M. E.; Bastien, I. J.; Baker, E. B. Stable Carbonium Ions. IV. Secondary and Tertiary Alkyl and Aralkyl Oxocarbonium Hexafluoroantimonates. Formation and Identification of the Trimethylcarbonium Ion by Decarbonylation of the *tert*-Butyl Oxocarbonium Ion. *J. Am. Chem. Soc.* **1963**, *85*, 1328−1334.
(9) Kato, T.; Reed, C. A. Putting *tert*-butyl cation in a bottle. *Angew. Chem., Int. Ed.* **2004**, *43*, 2908−2911.
(10) Yoder, R. A.; Johnston, J. N. A case study in biomimetic total synthesis: polyolefin carbocyclizations to terpenes and steroids. *Chem. Rev.* **2005**, *105*, 4730−4756.
(11) Fukuzawa, A.; Aye, M.; Nakamura, M.; Tanura, M.; Murai, A. Structure elucidation of laureoxanyne, a new nonisoprenoid C-15-enyne, using lactoperoxidase. *Tetrahedron Lett.* **1990**, *31*, 4895−4898.
(12) Kikuchi, H.; Suzuki, T.; Kurosawa, E.; Suzuki, M. The Structure of Notoryne, a Halogenated C15 Nonterpenoid with a Novel Carbon Skeleton from The Red Alga *Laurencia Nipponica* Yamada. *Bull. Chem. Soc. Jpn.* **1991**, *64*, 1763−1775.
(13) Murai, A. Biosynthesis of Cyclic Bromoethers from Red Algae. In *Comprehensive Natural Products Chemistry*; Barton, D. H. R., Meth-Cohn, O., Nakinishi, K., Eds.; Elsevier: Oxford, U.K., 1999; Vol. *1*, pp 303−324.
(14) Braddock, D. C. A hypothesis concerning the biosynthesis of the obtusallene family of marine natural products via electrophilic bromination. *Org. Lett.* **2006**, *8*, 6055−6058.
(15) Bonney, K. J.; Braddock, D. C. A unifying stereochemical analysis for the formation of halogenated C15-acetogenin medium-ring ethers from *Laurencia* species via intramolecular bromonium ion assisted epoxide ring-opening and experimental corroboration with a model epoxide. *J. Org. Chem.* **2012**, *77*, 9574−9584.
(16) Braddock, D. C.; Sbircea, D. T. Proof-of-principle direct double cyclisation of a linear C15-precursor to a dibrominated bicyclic medium-ring ether relevant to *Laurencia* species. *Chem. Commun.* **2014**, *50*, 12691−12693.
(17) Snyder, S. A.; Treitler, D. S.; Brucks, A. P.; Sattler, W. A general strategy for the stereocontrolled preparation of diverse 8- and 9-membered *Laurencia*-type bromoethers. *J. Am. Chem. Soc.* **2011**, *133*, 15898−15901.
(18) Zhang, Y. A.; Yaw, N.; Snyder, S. A. General Synthetic Approach for the *Laurencia* Family of Natural Products Empowered by a Potentially Biomimetic Ring Expansion. *J. Am. Chem. Soc.* **2019**, *141*, 7776−7788.
(19) Keshipeddy, S.; Martinez, I.; Castillo, B. F., 2nd; Morton, M. D.; Howell, A. R. Toward a formal synthesis of laureatin: unexpected rearrangements involving cyclic ether nucleophiles. *J. Org. Chem.* **2012**, *77*, 7883−7890.
(20) Dyson, B. S.; Burton, J. W.; Sohn, T. I.; Kim, B.; Bae, H.; Kim, D. Total synthesis and structure confirmation of elatenyne: success of computational methods for NMR prediction with highly flexible diastereomers. *J. Am. Chem. Soc.* **2012**, *134*, 11781−11790.
(21) Taylor, M. T.; Fox, J. M. Biosynthesis of the C15-acetogenin laurepoxide may involve bromine-induced skeletal rearrangement of a Δ4-oxocene precursor. *Tetrahedron Lett.* **2015**, *56*, 3560−3563.
(22) For recent reviews concerning *Laurencia* natural products see: (a) Wang, B. G.; Gloer, J. B.; Ji, N. Y.; Zhao, J. C. Halogenated organic molecules of Rhodomelaceae origin: Chemistry and Biology. *Chem. Rev.* **2013**, *113*, 3632−3685. (b) Zhou, Z. F.; Menna, M.; Cai, Y. S.; Guo, Y. W. Polyacetylenes of marine origin: chemistry and bioactivity. *Chem. Rev.* **2015**, *115*, 1543−1596. (c) Wanke, T.; Philippus, A. C.; Zatelli, G. A.; Vieira, L. F. O.; Lhullier, C.; Falkenberg, M. C_{15} acetogenins from the *Laurencia* complex: 50 years of research − an overview. *Rev. Bras. Farmacogn.* **2015**, *25*, 569−587.
(23) Fukuzawa, A.; Aye, M.; Takasugi, Y.; Nakamura, M.; Tamura, M.; Murai, A. Enzymatic Bromo-Ether Cyclization of Laurediols with Bromoperoxidase. *Chem. Lett.* **1994**, *23*, 2307−2310.
(24) Kim, B.; Lee, M.; Kim, M. J.; Lee, H.; Kim, S.; Kim, D.; Koh, M.; Park, S. B.; Shin, K. J. Biomimetic asymmetric total synthesis of (−)-laurefucin via an organoselenium-mediated intramolecular hydroxyetherification. *J. Am. Chem. Soc.* **2008**, *130*, 16807−16811.
(25) Clarke, J.; Bonney, K. J.; Yaqoob, M.; Solanki, S.; Rzepa, H. S.; White, A. J.; Millan, D. S.; Braddock, D. C. Epimeric face-selective oxidations and diastereodivergent transannular oxonium ion formation fragmentations: computational modeling and total syntheses of 12-epoxyobtusallene IV, 12-epoxyobtusallene II, obtusallene X, marilzabicycloallene C, and marilzabicycloallene D. *J. Org. Chem.* **2016**, *81*, 9539−9552.
(26) Kim, B.; Sohn, T. I.; Kim, D.; Paton, R. S. Asymmetric total syntheses and structure confirmation of chlorofucins and bromofucins. *Chem. - Eur. J.* **2018**, *24*, 2634−2642.
(27) Shepherd, E. D.; Dyson, B. S.; Hak, W. E.; Nguyen, Q. N. N.; Lee, M.; Kim, M. J.; Sohn, T. I.; Kim, D.; Burton, J. W.; Paton, R. S. Structure Determination of a Chloroenyne from *Laurencia majuscula* Using Computational Methods and Total Synthesis. *J. Org. Chem.* **2019**, *84*, 4971−4991.
(28) Snyder, S. A.; Brucks, A. P.; Treitler, D. S.; Moga, I. Concise synthetic approaches for the *Laurencia* family: formal total syntheses of (±)-laurefucin and (±)-*E*- and (±)-*Z*-pinnatifidenyne. *J. Am. Chem. Soc.* **2012**, *134*, 17714−17721.
(29) Kim, D.; Sohn, T.-i.; Kim, B.; Paton, R. S. Asymmetric Total Synthesis and Structure Confirmation of (+)-(3*E*)-Isolaurefucin Methyl Ether. *Heterocycles* **2018**, *97*, 179−191.
(30) Braddock, D. C.; Millan, D. S.; Perez-Fuertes, Y.; Pouwer, R. H.; Sheppard, R. N.; Solanki, S.; White, A. J. P. Bromonium Ion Induced Transannular Oxonium Ion Formation-Fragmentation in Model Obtusallene Systems and Structural Reassignment of Obtusallenes V-VII. *J. Org. Chem.* **2009**, *74*, 1835−1841.
(31) Stoyanov, E. S.; Gunbas, G.; Hafezi, N.; Mascal, M.; Stoyanova, I. V.; Tham, F. S.; Reed, C. A. The $R_3O^+ \bullet H^+$ hydrogen bond: toward a tetracoordinate oxadionium(2+) ion. *J. Am. Chem. Soc.* **2012**, *134*, 707−714.
(32) Fujiwara, K. Total Synthesis of Medium-Ring Ethers from *Laurencia* Red Algae. In *Marine Natural Products*; Kiyota, H., Ed.; Springer-Verlag: Berlin Heildelberg, 2006; Vol. *5*, pp 97−148.
(33) Murai, A.; Murase, H.; Matsue, H.; Masamune, T. The synthesis of (±)-Laurencin. *Tetrahedron Lett.* **1977**, *18*, 2507−2510.
(34) Masamune, T.; Matsue, H.; Murase, H. Synthetic Studies of Laurencin and Related Compounds. IV. Synthesis of *cis*-2-Ethyl-8-formyl-3,4,7,8-dihydro-2*H*-oxocin-3-one 3-Ethylene Acetal and Related Compounds. *Bull. Chem. Soc. Jpn.* **1979**, *52*, 127−134.
(35) Masamune, T.; Murase, H.; Matsue, H.; Murai, A. Synthetic Studies of Laurencin and Related Compounds. V. Transformation of *cis*-2-Ethyl-8-formyl-3,4,7,8-dihydro-2*H*-oxocin-3-one 3-Ethylene Acetal into (±)-Laurencin. *Bull. Chem. Soc. Jpn.* **1979**, *52*, 135−141.
(36) For reviews covering the synthesis of halogenated cyclic ether acetogenin natural products from *Laurencia* spp. see refs 22a and 32.

DOI: 10.1021/jacs.9b07438
J. Am. Chem. Soc. XXXX, XXX, XXX−XXX

(37) For biomimetic syntheses see refs 15−21 and 24−30.
(38) For selected recent non-biomimetic syntheses see: (a) Kim, B.; Sohn, T. I.; Kim, S.; Kim, D.; Lee, J. Concise Substrate-Controlled Asymmetric Total Synthesis of (+)-3-(*Z*)-Dihydrorhodophytin. *Heterocycles* **2010**, *82*, 1113−1118. (b) Kim, M. J.; Sohn, T. I.; Kim, D.; Paton, R. S. Concise substrate-controlled asymmetric total syntheses of dioxabicyclic marine natural products with 2,10-dioxabicyclo-[7.3.0]dodecene and 2,9-dioxabicyclo[6.3.0]undecene skeletons. *J. Am. Chem. Soc.* **2012**, *134*, 20178−20188. (c) Sohn, T. I.; Kim, D.; Paton, R. S. Substrate-Controlled Asymmetric Total Syntheses of Microcladallenes A, B, and C Based on the Proposed Structures. *Chem. - Eur. J.* **2015**, *21*, 15988−15997. (d) Yoshimura, F.; Okada, T.; Tanino, K. Asymmetric Total Synthesis of Laurallene. *Org. Lett.* **2019**, *21*, 559−562. Ref 27.
(39) For earlier notable contributions to the synthesis of halogenated ether acetogenins from *Laurencia* spp. see: (a) Overman, L. E.; Thompson, A. S. Total synthesis of (−)-laurenyne. Use of acetal-initiated cyclizations to prepare functionalized eight-membered cyclic ethers. *J. Am. Chem. Soc.* **1988**, *110*, 2248−2256. (b) Tsushima, K.; Murai, A. Total synthesis of (+)-laurencin. *Tetrahedron Lett.* **1992**, *33*, 4345−4348. (c) Lee, E.; Park, C. M.; Yun, J. S. Total Synthesis of Dactomelynes. *J. Am. Chem. Soc.* **1995**, *117*, 8017−8018. (d) Burton, J. W.; Clark, J. S.; Derrer, S.; Stork, T. C.; Bendall, J. G.; Holmes, A. B. Synthesis of medium ring ethers. 5. The synthesis of (+)-laurencin. *J. Am. Chem. Soc.* **1997**, *119*, 7483−7498. (e) Crimmins, M. T.; Choy, A. L. An Asymmetric Aldol-Ring-Closing Metathesis Strategy for the Enantioselective Construction of Oxygen Heterocycles: An Efficient Approach to the Enantioselective Synthesis of (+)-Laurencin. *J. Am. Chem. Soc.* **1999**, *121*, 5653−5660. (f) Fujiwara, K.; Awakura, D.; Tsunashima, M.; Nakamura, A.; Honma, T.; Murai, A. Total Synthesis of (+)-Obtusenyne. *J. Org. Chem.* **1999**, *64*, 2616−2617. (g) Kim, H.; Choi, W. J.; Jung, J.; Kim, S.; Kim, D. Construction of eight-membered ether rings by olefin geometry-dependent internal alkylation: First asymmetric total syntheses of (+)-3-(*E*)- and (+)-3-(*E*)-pinnatifidenyne. *J. Am. Chem. Soc.* **2003**, *125*, 10238−10240.
(40) Fukuzawa, A.; Aye, M.; Murai, A. A Direct Enzymatic Synthesis of Laurencin from Laurediol. *Chem. Lett.* **1990**, *19*, 1579−1580.
(41) Kurosawa, E.; Irie, T.; Fukuzawa, A. *trans*-Laurediol and *cis*-laurediol, unsaturated glycols from *Laurencia Nipponica* yamada. *Tetrahedron Lett.* **1972**, *13*, 2121−2124.
(42) Fukuzawa, A.; Honma, T.; Takasugi, Y.; Murai, A. Biogenetic intermediates, (3*E* and 3*Z*,12*Z*)-laurediols and (3*E* and 3*Z*)-12,13-dihydrolaurediols, isolated from *Laurencia Nipponica*. *Phytochemistry* **1993**, *32*, 1435−1438.
(43) For reviews of halogenating enzymes see: (a) Butler, A.; Carter-Franklin, J. N. The role of vanadium bromoperoxidase in the biosynthesis of halogenated marine natural products. *Nat. Prod. Rep.* **2004**, *21*, 180−188. (b) Vaillancourt, F. H.; Yeh, E.; Vosburg, D. A.; Garneau-Tsodikova, S.; Walsh, C. T. Nature's inventory of halogenation catalysts: Oxidative strategies predominate. *Chem. Rev.* **2006**, *106*, 3364−3378.
(44) Kaneko, K.; Washio, K.; Umezawa, T.; Matsuda, F.; Morikawa, M.; Okino, T. cDNA cloning and characterization of vanadium-dependent bromoperoxidases from the red alga *Laurencia nipponica*. *Biosci., Biotechnol., Biochem.* **2014**, *78*, 1310−1319.
(45) Davies, S. G.; Polywka, M. E. C.; Thomas, S. E. Stereoselective synthesis of cyclic ethers via bromine assisted epoxide ring expansion. *Tetrahedron Lett.* **1985**, *26*, 1461−1464.
(46) Suzuki proposed a different route from laurediol to prelaurefucin; see ref 12.
(47) For previous syntheses of notoryne see: Senapati, S.; Das, S.; Ramana, C. V. Total Synthesis of Notoryne. *J. Org. Chem.* **2018**, *83*, 12863−12868 and ref 27 .
(48) Laurefucin. Isolation and structure determination: (a) Fukuzawa, A.; Kurosawa, E.; Irie, T. Laurefucin and acetyllaurefucin, new bromo compounds from *Laurencia Nipponica* yamada. *Tetrahedron Lett.* **1972**, *13*, 3−6. (b) Furusaki, A.; Kurosawa, E.; Fukuzawa, A.; Irie, T. The revised structure and absolute configuration of Laurefucin from *Laurencia Nipponica* Yamada. *Tetrahedron Lett.* **1973**, *14*, 4579−4582. Reisolation: (c) Wratten, S. J.; Faulkner, D. J. Metabolites of the red alga *Laurencia subopposita*. *J. Org. Chem.* **1977**, *42*, 3343−3349. Previous synthesis see refs 24 and 28.
(49) For isolation and structure determination of acetyllaurefucin see refs 48a−c.
(50) Bromofucins. Isolation: (a) Coll, J. C.; Wright, A. D. Tropical Marine-Algae. IV. Novel Metabolites from the Red Alga *Laurencia implicata* (Rhodophyta, Rhodophyceae, Ceramiales, Rhodomelaceae). *Aust. J. Chem.* **1989**, *42*, 1685−1693. (b) McPhail, K. L.; Davies-Coleman, M. T. (3*Z*)-bromofucin from a South African sea hare. *Nat. Prod. Res.* **2005**, *19*, 449−452. (c) Suzuki, M.; Takahashi, Y.; Matsuo, Y.; Masuda, M. Pannosallene, a brominated C-15 nonterpenoid from *Laurencia pannosa*. *Phytochemistry* **1996**, *41*, 1101−1103. Synthesis: ref 25.
(51) Chlorofucins. Isolation: (a) Howard, B. M.; Schulte, G. R.; Fenical, W.; Solheim, B.; Clardy, J. Three new vinyl acetylenes from the marine red alga. *Tetrahedron* **1980**, *36*, 1747−1751. (b) Denys, R.; Coll, J. C.; Carroll, A. R.; Bowden, B. F. Tropical marine-algae. X. Isolaurefucin methyl-ether, a new lauroxocane derivative from the red alga *Dasyphila-Plumariodes*. *Aust. J. Chem.* **1993**, *46*, 1073−1077. (c) Suzuki, M.; Daitoh, M.; Vairappan, C. S.; Abe, T.; Masuda, M. Novel halogenated metabolites from the Malaysian *Laurencia pannosa*. *J. Nat. Prod.* **2001**, *64*, 597−602. Synthesis: ref 25.
(52) Elatenynes. Isolation and structure determination: (a) Hall, J. G.; Reiss, J. A. Elatenyne − a Pyrano[3,2-*b*]pyranyl Vinyl Acetylene from the Red Alga. *Aust. J. Chem.* **1986**, *39*, 1401−1409. (b) Kim, I. K.; Brennan, M. R.; Erickson, K. L. Lauroxolanes from the marins alga *Laurencia Majuscula*. *Tetrahedron Lett.* **1989**, *30*, 1757−1760. (c) Sheldrake, H. M.; Jamieson, C.; Burton, J. W. The changing faces of halogenated marine natural products: Total synthesis of the reported structures of elatenyne and an enyne from *Laurencia majuscula*. *Angew. Chem., Int. Ed.* **2006**, *45*, 7199−7202. (d) Smith, S. G.; Paton, R. S.; Burton, J. W.; Goodman, J. M. Stereostructure assignment of flexible five-membered rings by GIAO (13)C NMR calculations: Prediction of the stereochemistry of elatenyne. *J. Org. Chem.* **2008**, *73*, 4053−4062. (e) Dias, D. A.; Urban, S. Phytochemical studies of the southern Australian marine alga, *Laurencia elata*. *Phytochemistry* **2011**, *72*, 2081−2089. Ref 17. (f) Urban, S.; Brkljaca, R.; Hoshino, M.; Lee, S.; Fujita, M. Determination of the Absolute Configuration of the Pseudo-Symmetric Natural Product Elatenyne by the Crystalline Sponge Method. *Angew. Chem., Int. Ed.* **2016**, *55*, 2678−2682. Synthesis: ref 20.
(53) Laurendecumenyne B. Isolation and structure determination: (a) Ji, N. Y.; Li, X. M.; Li, K.; Wang, B. G. Laurendecumallenes A-B and laurendecumenynes A-B, halogenated nonterpenoid C-15-Acetogenins from the marine red alga *Laurencia decumbens*. *J. Nat. Prod.* **2007**, *70*, 1499−1502. (b) Ji, N. Y.; Li, X. M.; Li, K.; Wang, B. G. *J. Nat. Prod.* **2007**, *70*, 1499; *J. Nat. Prod.* **2010**, *73*, 1192. (c) Ref 20. Synthesis ref 20.
(54) Schulte, G. R.; Chung, M. C. H.; Scheuer, P. J. Two bicyclic C15 enynes from the sea hare *Aplysia oculifera*. *J. Org. Chem.* **1981**, *46*, 3870−3873.
(55) Jeong, D.; Sohn, T. I.; Kim, J. Y.; Kim, G.; Kim, D.; Paton, R. S. Construction of 6,10-*syn*- and -*anti*-2,5-dioxabicyclo[2.2.1]heptane skeletons via oxonium ion formation/fragmentation: prediction of structure of (*E*)-ocellenyne by NMR calculation. *Org. Lett.* **2017**, *19*, 6252−6255.
(56) Olah, G. A.; Laali, K. K.; Wang, Q.; Prakash, G. K. S. *Onium Ions*; Wiley: New York, 1998.
(57) Krossing, I. The facile preparation of weakly coordinating anions: structure and characterisation of silverpolyfluoroalkoxyaluminates $AgAl(OR_F)_4$, calculation of the alkoxide ion affinity. *Chem. - Eur. J.* **2001**, *7*, 490−502.
(58) Braddock, D. C.; Hermitage, S. A.; Kwok, L.; Pouwer, R.; Redmond, J. M.; White, A. J. The generation and trapping of enantiopure bromonium ions. *Chem. Commun.* **2009**, 1082−1084.
(59) The relative configuration of the dioxabicyclo[5.2.1]decanes **28**, *ent*-(*E*/*Z*)-**29**, *ent*-**15**, *ent*-(*Z*)-**16**, (*E*/*Z*)-**19**, (*E*/*Z*)-**24** and the

DOI: 10.1021/jacs.9b07438
J. Am. Chem. Soc. XXXX, XXX, XXX−XXX

oxonium ions *ent*-(*E*/*Z*)-**13**·Al(pftb)$_4$ and (*E*/*Z*)-**20**·Al(pftb)$_4$, **46**·Al(pftb)$_4$ were assigned by ^{1}H NMR NOE experiments including ROSEY where necessary (Supporting Information section 14, pp S77−S84). For the natural products (*E*/*Z*)-**19**, (*E*/*Z*)-**24**, *ent*-(*E*)-**16**, *ent*-(*E*/*Z*)-**14**, (*Z*)-**21**, (*E*/*Z*)-**22**, and α,β-unsaturated aldehydes **36** and **40** comparison with literature data confirmed their structures (Supporting Information, pp S26−S28 and sections 10 and 11, pp S60−S76).

(60) Stork, G.; Zhao, K. A stereoselective synthesis of (*Z*)-1-iodo-1-alkenes. *Tetrahedron Lett.* **1989**, *30*, 2173−2174.

(61) Voigtritter, K.; Ghorai, S.; Lipshutz, B. H. Rate enhanced olefin cross-metathesis reactions: the copper iodide effect. *J. Org. Chem.* **2011**, *76*, 4697−4702.

(62) Etzkorn, M.; Aniszfeld, R.; Li, T.; Buchholz, H.; Rasul, G.; Prakash, G. K. S.; Olah, G. A. 1-Oxoniaadamantane. *Eur. J. Org. Chem.* **2008**, *2008*, 4555−4558.

(63) Mascal, M.; Hafezi, N.; Meher, N. K.; Fettinger, J. C. Oxatriquinane and oxatriquinacene: extraordinary oxonium ions. *J. Am. Chem. Soc.* **2008**, *130*, 13532−13533.

(64) Molecular mechanics conformational searches were performed with *Spartan16*; Wavefunction, Inc.: Irvine, CA. DFT optimizations with several functionals were performed with *Gaussian09*, rev. D.01; Gaussian, Inc.: Wallingford, CT, 2016. Computational methods and references are described in full in the Supporting Information.

(65) For related 1,2-hydride shifts involving oxonium ions see: Sugimoto, M.; Suzuki, T.; Hagiwara, H.; Hoshi, T. The first total synthesis of (+)-(*Z*)-laureatin. *Tetrahedron Lett.* **2007**, *48*, 1109−1112 and refs 17 and 24 .

(66) A referee suggested the oxocarbenium ion may be formed by elimination to give an enol ether followed by C-protonation. We cannot rule out this mechanism as it would have the same kinetic profile as the proposed 1,2-hydride shift if enol ether protonation was fast with respect to elimination. We favor the illustrated 1,2-hydride shift due to precedent in related systems (ref 65) and the computational analysis (Figure 4).

(67) Sohn, T.; Kim, M. J.; Kim, D. Asymmetric Total Synthesis of Trilobacin via Organoselenium-Mediated Oxonium Ion Formation/SiO_2-Promoted Fragmentation. *J. Am. Chem. Soc.* **2010**, *132*, 12226−12227.

(68) The DFT calculations on the opening of oxonium ions *ent*-(*E*)-**13** and (*E*)-**20** expand upon the recently reported studies of the opening of closely related oxonium ions (truncated versions of **13** and **20**) with water (ref 29). The current study (Figures 5 and S36−S48) uses water and chloride as nucleophiles, on the complete substrates, at several levels of theory, with distortion-interaction/activation-strain analysis to analyze the preference for opening at C-7, C-10, and C-13 with both *ent*-(*E*)-**13** and (*E*)-**20**.

(69) Bickelhaupt, F. M.; Houk, K. N. Analyzing Reaction Rates with the Distortion/Interaction-Activation Strain Model. *Angew. Chem., Int. Ed.* **2017**, *56*, 10070−10086.

(70) Tantillo, D. J. Importance of Inherent Substrate Reactivity in Enzyme-Promoted Carbocation Cyclization/Rearrangements. *Angew. Chem., Int. Ed.* **2017**, *56*, 10040−10045.

DOI: 10.1021/jacs.9b07438
J. Am. Chem. Soc. XXXX, XXX, XXX−XXX